

# The Spin Period of EX Hydrae

A.R. King & G.A. Wynn,

*Astronomy Group, University of Leicester, Leicester, LE1 7RH*

12 July 2021

## ABSTRACT

We show that the spin period of the white dwarf in the magnetic CV EX Hydrae represents an equilibrium state in which the corotation radius is comparable with the distance from the white dwarf to the inner Lagrange point. We also show that a continuum of spin equilibria exists at which  $P_{\text{spin}}$  is significantly longer than  $\sim 0.1P_{\text{orb}}$ . Most systems occupying these equilibrium states should have orbital periods below the CV period gap, as observed.

**Key Words:** accretion, accretion discs - binaries: close - stars: individual: EX Hydrae - stars: magnetic fields.

## 1 INTRODUCTION

Cataclysmic variables (CVs) are semi-detached binaries in which a low-mass, main-sequence secondary star transfers mass to a white dwarf. In a significant number of systems the white dwarf has a magnetic moment strong enough to channel the accretion flow on to restricted regions of its surface; such systems are known as magnetic CVs. Observationally these systems are characterized by the presence of two coherent periods  $P_{\text{orb}}$ ,  $P_{\text{spin}}$ , corresponding to the orbital rotation of the binary and the white dwarf spin respectively. Sometimes the beat period

$$P_{\text{beat}} = (P_{\text{spin}}^{-1} - P_{\text{orb}}^{-1})^{-1} \quad (1)$$

is seen in addition to or even in place of  $P_{\text{spin}}$ . Magnetic CVs are interesting because the white dwarf spin rates give insight into the angular momentum flows within the binary. These flows are more complex than in the analogous systems (pulsing X-ray binaries) in which the accretor is a magnetic neutron star, simply because the white dwarf magnetic moments  $\mu_1$  ( $\gtrsim 10^{33}$  G cm<sup>3</sup>) are much larger than those of the neutron stars ( $\mu_1 \lesssim 10^{30}$  G cm<sup>3</sup>). Accordingly the magnetospheric radius in a magnetic CV is a significant fraction of the binary separation  $a$ , whereas it is far smaller in the neutron-star case. As an illustration of this, the white dwarf spin can be locked to the binary rotation ( $P_{\text{spin}} = P_{\text{orb}}$ ) in some magnetic CVs (called AM Her stars), while  $P_{\text{spin}}$  is always considerably smaller than  $P_{\text{orb}}$  in neutron-star systems.

Historically the neutron-star systems were discovered first, and simple theories of the angular momentum flows were developed for them (e.g. Ghosh & Lamb, 1979). There has been a natural tendency to transfer these theories bodily to the white dwarf case, even though the larger magnetic moments make this very questionable. In particular, neutron-star magnetospheres are so small that Roche lobe overflow must always lead to the formation of a Keplerian accretion disc in the standard way (e.g. Frank et al., 1992). By contrast, a white dwarf magnetic field can have a strong

influence on the accretion flow at all radii, making it non-Keplerian even though it may surround the white dwarf. This in turn tends to lead to an equilibrium spin rate determined approximately by the condition (King, 1993; Wynn & King, 1995)

$$R_{\text{co}} \sim R_{\text{circ}}. \quad (2)$$

Here

$$R_{\text{co}} = \left( \frac{GM_1 P_{\text{spin}}^2}{4\pi^2} \right)^{1/3} \quad (3)$$

is the corotation radius, at which matter in local Kepler rotation about a white dwarf of mass  $M_1$  corotates with the magnetic field lines, and  $R_{\text{circ}}$  is the circularization radius, i.e. the radius at which the Kepler specific angular momentum equals that of matter accreting through the inner Lagrange point  $L_1$ . If the latter is a distance  $b$  from the white dwarf we can find an approximation for  $R_{\text{circ}}$  by equating the specific angular momentum  $\sim b^2(2\pi/P_{\text{orb}})$  at  $L_1$  to the specific Kepler angular momentum at  $R_{\text{circ}}$  (this neglects the effects of the companion)

$$R_{\text{circ}} \simeq \frac{M}{M_1} \left( \frac{b}{a} \right)^4 \left( \frac{GM P_{\text{orb}}^2}{4\pi^2} \right)^{1/3}, \quad (4)$$

where  $M = M_1 + M_2$  is the total binary mass. Numerical fits to Roche geometry give

$$\frac{b}{a} = 0.500 - 0.227 \log \frac{M_2}{M_1} \quad (5)$$

(Warner 1976). Hence combining (2 - 5) gives a spin equilibrium

$$\frac{P_{\text{spin}}}{P_{\text{orb}}} \sim \left( \frac{b}{a} \right)^6 \left( \frac{M}{M_1} \right)^2 \sim 0.07 \quad (6)$$

for typical mass ratios (cf King, 1993, Wynn & King, 1995). The numerical simulations performed by Wynn & King (1995) used the magnetic drag prescription introduced by King (1993). Here the flow is assumed to be in the form of diamagnetic blobs, the local magnetic field  $B = \mu_1/r^3$

acting on them through a surface drag. This produces an acceleration

$$\mathbf{f}_{\text{mag}} = -k[\mathbf{v} - \mathbf{v}_f]_{\perp}, \quad (7)$$

where  $\mathbf{v}$  and  $\mathbf{v}_f$  are the blob and field velocities (i.e.  $v_f = 2\pi r/P_{\text{spin}}$ ), the suffix  $\perp$  denotes the velocity components perpendicular to the field lines, and  $k = t_{\text{mag}}^{-1}$ , with  $t_{\text{mag}}$  the drag time scale given by

$$t_{\text{mag}} \simeq \frac{c_A \rho_b l_b}{B^2} \quad (8)$$

(Drell, Foley and Ruderman, 1965). Here  $\rho_b, l_b$  are the blob density and length scale, and  $c_A$  is the Alfvén speed in the inter-blob plasma. Thus as the blobs move through the magnetosphere they exchange orbital energy and angular momentum with the white dwarf via the drag term. The blob parameters  $\rho_b, l_b$  are to some extent arbitrary, but limited for example by physical conditions near  $L_1$ . Numerical simulation of the flow including the full Roche potential rather than the simple approximation (4) examined the regime in which

$$t_{\text{mag}}(R_{\text{circ}}) \sim t_{\text{dyn}}(R_{\text{circ}}), \quad (9)$$

or alternatively

$$t_{\text{mag}}(L_1) \gg t_{\text{dyn}}(L_1), \quad (10)$$

where  $t_{\text{dyn}} \sim (r^3/GM_1)^{1/2}$  is the dynamical time scale. These simulations give similar but slightly larger values of  $P_{\text{spin}}/P_{\text{orb}}$  to the approximation (6).

Equation (6) reasonably describes the relation between  $P_{\text{spin}}$  and  $P_{\text{orb}}$  in most non-synchronous magnetic CVs ('intermediate polars', or IPs). The corresponding accretion flow is sometimes referred to as 'discless'. This is a rather misleading name, suggesting for example that the flow cannot surround the white dwarf, although simulations show that this is possible (Fig. 1). Observations suggesting for example that matter is fed to the white dwarf at all spin phases are sometimes taken as evidence against this type of accretion. However the fundamental property of this flow is not the absence of matter surrounding the white dwarf, but simply the non-Keplerian nature of the velocity field. This in turn reflects the pervasive influence of the magnetic field on the accretion dynamics. The divergence from Keplerian flow is a manifestation of the complex angular momentum flow within the system, where the angular momenta of the blobs may be transferred to the primary star via the field or accretion, recaptured by the secondary star or lost to the binary entirely. This contrasts with the case of a Keplerian accretion disc where the angular momentum transferred through  $L_1$  is passed back to the binary orbit via tidal forces at the outer edge of the disc.

Since the IPs cover a large range of magnetic field and orbital period there are several exceptions to the equilibrium represented by (6). One would expect systems with Keplerian discs to have  $R_{\text{co}} < R_{\text{circ}}$  and thus a smaller ratio  $P_{\text{spin}}/P_{\text{orb}}$  than given by (6). This appears to be the case in at least two systems. In GK Per ( $P_{\text{spin}} = 381$  s,  $P_{\text{orb}} = 48$  hr) the orbital period is so long that the magnetospheric radius is small compared with  $R_{\text{circ}}$ , so a Keplerian disc will form in the standard way. In DQ Her ( $P_{\text{spin}} = 71$  s,  $P_{\text{orb}} = 4.65$  hr) the very short spin period presumably indicates a rather low magnetic field, leading to the same conclusion. How-

ever, the still shorter spin period of AE Aqr ( $P_{\text{spin}} = 33$  s,  $P_{\text{orb}} = 9.88$  hr) does *not* imply a Keplerian disc (Wynn, King & Horne, 1997, and references therein); here the matter transferred from the secondary star is apparently being centrifugally ejected, showing that disc formation depends on  $P_{\text{spin}}$  as well as the magnetic moment  $\mu_1$  (cf. equation 7).

In addition to the systems with  $P_{\text{spin}}/P_{\text{orb}}$  smaller than implied by (6) there are two IPs with a much larger ratio: EX Hya has  $P_{\text{spin}} = 67$  min,  $P_{\text{orb}} = 98$  min, and RX1238-38 has  $P_{\text{spin}} = 36$  min,  $P_{\text{orb}} = 90$  min. This clearly does not fit the 'IP' spin equilibrium (6), still less the equilibrium expected for accretion from a Keplerian disc. A spin period far from equilibrium would imply that we are seeing these systems in a very short-lived phase: in the case of EX Hya the spin period derivative is  $\dot{P}_{\text{spin}} = -3.8 \times 10^{-11}$  s s $^{-1}$  (eg. Warner, 1995), with a spindown timescale of  $\sim 10^6$  y, much shorter than the orbital evolution timescale ( $\gtrsim 10^8$  y). It is far more likely that the spin is currently close to equilibrium, but that this equilibrium differs from that represented by (6) or the Keplerian case. In this paper we shall show that EX Hya represents a new type of spin equilibrium for IPs with short orbital periods.

## 2 SPIN EQUILIBRIUM IN EX HYDRAE

Most IPs so far discovered have orbital periods on the long side of the CV period gap  $2 \text{ hr} \lesssim P_{\text{orb}} \lesssim 3 \text{ hr}$ . EX Hya's short orbital period is therefore very suggestive: if its magnetic field is similar to systems conforming to (6) we would expect the smaller orbital separation and lower mass transfer rate to make the effective magnetospheric radius comparable with the distance to the secondary star. Here magnetic forces will dominate the motion of the gas blobs near  $L_1$  and

$$t_{\text{mag}}(L_1) \lesssim t_{\text{dyn}}(L_1). \quad (11)$$

Setting  $\rho_b$  and  $l_b$  to be equal to the expected stream density ( $\sim 10^{-9}$  g cm $^{-3}$ ) and width ( $\sim 10^9$  cm) at  $L_1$  respectively, we find  $t_{\text{mag}}(L_1) \sim t_{\text{dyn}}(L_1)$  for  $\mu_1(\text{crit}) \sim 3 \times 10^{33}$  G cm $^3$  (cf fig. 6). For magnetic moments larger than this we might then expect to see the equilibrium condition (2) (which leads to eq. 6) replaced by

$$R_{\text{co}} \sim b, \quad (12)$$

leading (from 3, 5) to

$$\frac{P_{\text{spin}}}{P_{\text{orb}}} \sim \left(\frac{b}{a}\right)^{3/2} = \left(0.500 - 0.227 \log \frac{M_2}{M_1}\right)^{3/2}. \quad (13)$$

For the mass ratio  $M_2/M_1 = 0.19$  (Hellier, 1996) appropriate to EX Hya we find  $P_{\text{spin}}/P_{\text{orb}} \sim 0.54$ , similar to the measured  $P_{\text{spin}}/P_{\text{orb}} = 0.68$ . However this simple treatment completely neglects the full Roche potential. Since the angular momentum exchange determining  $P_{\text{spin}}/P_{\text{orb}}$  in this type of flow occurs near  $L_1$  we expect a significant modification of this result because of the presence of the secondary star (this effect was less serious for the IP equilibrium (6) as the angular momentum exchange there occurs much closer to the white dwarf). We therefore need numerical simulations using the full Roche potential.

Clearly the condition (11) favours larger values of the magnetic moment  $\mu_1$ . However this must not be so large

that the system synchronizes and becomes an AM Her system. This condition can be expressed as (e.g. King, Frank & Whitehurst, 1991)

$$\frac{\mu_1 \mu_2}{a^3} < \frac{2\pi \dot{M} b^2}{P_{\text{orb}}}, \quad (14)$$

where  $\mu_2$  is the secondary dipole and  $\dot{M}$  is the mass transfer rate. In practice this condition requires

$$\mu_1 \lesssim 10^{34} \text{ G cm}^3. \quad (15)$$

Spin evolution calculations similar to those of Wynn and King (1995) show that the spin period of the white dwarf in EX Hya reaches an equilibrium which is in excellent agreement with the observed  $P_{\text{spin}}/P_{\text{orb}} = 0.68$  ratio, for  $t_{\text{mag}}(L_1)/t_{\text{dyn}}(L_1) \lesssim 1/3$  (see section 3 and figure 5). Spin equilibrium was attained on a time-scale  $t_{\text{spin}} \sim 10^7$  yrs, much shorter than the orbital evolution time-scale. This numerical result contrasts with the simple estimate above which predicted a ratio of  $P_{\text{spin}}/P_{\text{orb}} = 0.54$  from the white dwarf potential alone. We conclude that (12) indeed specifies a spin equilibrium state, and that EX Hya is close to this state.

Figure 2 shows a sequence of views of the accretion flow in the equilibrium spin state of our model system. This suggests that accretion of mass and angular momentum by the white dwarf occurs only for a restricted range of spin phases, essentially when the dipole axis points towards  $L_1$ . At other phases the condition (12) shows that matter trying to accrete along field lines will be centrifugally ejected. Much of this ejecta will be re-accreted by the secondary, transferring angular momentum from the white dwarf back to the binary orbit. In equilibrium these angular momentum flows balance over each orbit. We note here that recent spectroscopic observations (Wynn, Wheatley and Maxted, 1999) show strong evidence for just this sort of flow pattern in EX Hya. Figure 3 shows the fractions of mass transferred instantaneously through  $L_1$  which are accreted, returned to the companion star, or ejected entirely from the system for the simulation depicted in figure 2. It can clearly be seen that most of the transferred mass is accreted by the white dwarf, and this accretion occurs in two 'bursts' each beat cycle. It should be noted however, that the simulation takes no account of the modulation of the accretion flux by the white dwarf spin which may well dominate the observed light curve.

The spin equilibrium described here is quite robust and, in particular, may be achieved with a large spread in blob parameters: only  $\sim 25\%$  of the accreting mass need be magnetically dominated (i.e. condition 11 holds) to achieve the EX Hya equilibrium. Figure 4 shows the results of a simulation with a greater spread in blob parameters. In this figure it is clear that the accretion flow consists of 2 components, one of which is similar to that described above and the other is a azimuthally symmetric distribution of particles surrounding the white dwarf. This complex system could mimic many of the observational properties expected of accretion via a disc and via a stream, whilst still attaining an equilibrium  $P_{\text{spin}}/P_{\text{orb}}$  ratio very close to that observed for EX Hya.

### 3 A CONTINUUM OF SPIN EQUILIBRIA

The equilibrium conditions (2) and (12) suggest that there exists a continuum of equilibrium states in which

$$R_{\text{circ}} \lesssim R_{\text{co}} \lesssim b. \quad (16)$$

Figure 5 shows this set of equilibrium states for various values of  $t_{\text{mag}}(L_1)/t_{\text{dyn}}(L_1)$ , in the case of a binary with system parameters identical to those of EX Hya. Using (8) to provide an estimate of  $\mu_1$  from  $t_{\text{mag}}(L_1)$  it can be seen that the equilibrium states between the usual IP equilibrium

$$P_{\text{spin}}/P_{\text{orb}} \sim 0.1, \quad 5 \times 10^{30} \text{ G cm}^3 \lesssim \mu_1 \lesssim 10^{31} \text{ G cm}^3 \quad (17)$$

and the EX Hya equilibrium

$$P_{\text{spin}}/P_{\text{orb}} \sim 0.68, \quad 10^{33} \text{ G cm}^3 \lesssim \mu_1 \lesssim 10^{34} \text{ G cm}^3 \quad (18)$$

(with the exact value of each depending upon the mass ratio of the system) are defined by

$$0.1 \lesssim P_{\text{spin}}/P_{\text{orb}} \lesssim 0.68, \quad 10^{31} \text{ G cm}^3 \lesssim \mu_1 \lesssim 10^{33} \text{ G cm}^3. \quad (19)$$

For  $\mu_1 \lesssim 5 \times 10^{30} \text{ G cm}^3$  a standard Keplerian accretion disc would be expected to form, and for  $\mu_1 \gtrsim 10^{34} \text{ G cm}^3$  the system would synchronize and be observable as an AM Her star. Primary magnetic moments  $\lesssim 10^{31} \text{ G cm}^3$  are much lower than those normally inferred for IPs above the period gap ( $\gtrsim 10^{32} \text{ G cm}^3$ ). Therefore, we would expect IPs above the period gap to evolve into EX Hya-like systems or AM Hers. It should be noted that each system would have a unique curve similar to that presented in figure 5, which would be a function of  $P_{\text{orb}}$ ,  $M_2/M_1$  and  $\dot{M}$ .

The spin period of the white dwarf in the short period magnetic CV RX1238-38 ( $P_{\text{spin}}/P_{\text{orb}} \simeq 0.4$ ) may represent one of these continuum equilibrium states. Confirmation of this is dependent on the (as yet undetermined) mass ratio of the system. However, the  $P_{\text{spin}}/P_{\text{orb}}$  ratio is clearly too high to represent the usual IP equilibrium 6. If  $P_{\text{spin}}$  was determined by  $R_{\text{co}} \sim b$  then (13) gives a rough estimate of the mass ratio of the system as  $M_2/M_1 \sim 0.65$ . This mass ratio is rather high for a system below the period gap and the most likely possibility is that RX1238-38 represents one of the possible spin equilibria defined by (16).

### 4 DISCUSSION

The reasoning above shows that EX Hya represents a new equilibrium spin state for magnetic CVs characterized by the approximate equality (12). We can now show that the necessary conditions (11, 15) generally confine this equilibrium state to short orbital periods, in precise agreement with observation. In Figure 6 we plot  $t_{\text{mag}}(L_1)/t_{\text{dyn}}(L_1)$  versus  $P_{\text{orb}}$  for three values of  $\mu_1$ . (We have assumed secular mean values for  $M_2, \dot{M}$ , cf e.g. King, 1988.) Evidently the required conditions for the EX Hya equilibrium hold only for a narrow range

$$2 \times 10^{33} \text{ G cm}^3 \lesssim \mu_1 \lesssim 10^{34} \text{ G cm}^3, \quad (20)$$

(in agreement with Figure 6), and then only for

$$P_{\text{orb}} < 2 \text{ hr}, \quad (21)$$

i.e. periods below the gap. For (11) to hold at periods above the gap would require values of  $\mu_1$  probably violating (15),

i.e. such systems are generally synchronous (AM Her systems). Thus we expect most systems in this equilibrium state to be below the period gap.

There is a continuum of equilibrium spin states which connect the usual IP equilibrium and that represented by EX Hya. The spin equilibrium for a given  $P_{\text{orb}}$ ,  $M_2/M_1$  and  $\dot{M}$  is determined by the strength of the primary's magnetic moment. The other short period magnetic CV RX1238-38 most likely occupies one of these states. The relatively low values of  $\mu_1$  ( $\gtrsim 10^{31}$  g cm<sup>3</sup>) required to attain such equilibria at short orbital periods ( $\lesssim 2$  hr) indicates that magnetic CVs above the orbital period gap will evolve toward long spin periods (either  $P_{\text{spin}} > 0.1P_{\text{orb}}$ , or  $P_{\text{spin}} = P_{\text{orb}}$ ) below the gap. It is possible that some of these longer spin equilibria may be attainable above the period gap.

We may now crudely classify magnetic CVs according to  $P_{\text{orb}}$  and  $\mu_1$  (Fig. 9). We see that EX Hya-type systems have field strengths similar to typical IPs above the period gap and comparable with the weakest-field AM Her systems below it. Systems with larger  $\mu_1$  are evidently AM Her systems below the gap even if not above it. The Figure prompts the obvious question as to why there are so few asynchronous magnetic CVs below the period gap. There are a number of possibilities:

(i) the field distribution has a lower bound, and such systems are rare. DQ Her would be an example above the period gap.

(ii) Such systems do exist, but are difficult to detect, particularly below the period gap.

(iii) Orbital angular momentum losses associated with the ejected material drive the orbital evolution of short period systems significantly more quickly than gravitational radiation alone.

In the second case, we should remember that IPs are usually found through their medium-energy ( $\gtrsim 2$  keV) emission. The lower mass transfer rates below the period gap may simply make this too weak for detection.

We have shown that the spin period of EX Hya corresponds to a new equilibrium state in which the corotation radius is comparable to the distance to the inner Lagrange point. Moreover this equilibrium is only likely below the period gap, because the magnetic fields required above the gap would make the systems synchronous. The accretion flow (Fig. 1) characterizing this state has distinctive features which should allow observational tests. We note that Wynn, Wheatley and Maxted (1999) present data which provide strong evidence for exactly this form of accretion/ejection flow in EX Hya.

## 5 ACKNOWLEDGMENTS

Research in theoretical astrophysics at the University of Leicester is supported by a PPARC rolling grant. ARK gratefully acknowledges a PPARC Senior Fellowship.

## REFERENCES

Drell S.D., Foley H.M., Ruderman M.A., 1965, *J. Geophys. Res.*, 70, 3131

Frank J., King A.R., Raine D.J., 1992, *Accretion power in Astrophysics*, 2nd edn. Cambridge Univ. Press, Cambridge

Ghosh P. and Lamb F.K., 1979, *Ap.J.*, 232, 259

Hellier C., in Evans A. and Wood J. H., eds, *Cataclysmic Variables and Related Objects*,

King A.R., 1988, *QJRAS*, 29, 1

King A.R., 1993, *MNRAS*, 261, 144

King A.R., Frank, J., Whitehurst, R., 1991, *MNRAS* 250, 152

Warner, B., 1976, in Eggleton P., Mitton S., Whelan J., eds, *Proc IAU Symp 73, Structure and Evolution of Close Binary Systems*, Reidel, Dordrecht, p. 85

Warner, B., 1995, *Cataclysmic Variable Stars*, Cambridge Univ. Press, Cambridge

Wynn G.A., King A.R., 1995, *MNRAS*, 275, 9

Wynn G.A., King A.R., Horne, K., 1997, *MNRAS* 286, 436

Wynn G.A., Wheatley P.J., Maxted P., 1999, in prep

## Figure Captions

**Figure 1** Numerical simulations of the accretion flow in EX Hya, adopting the magnetic drag prescription of King (1993), and a dipolar magnetic field geometry. The upper panels depict the system as viewed from above the orbital (x-y) plane, where the motion of the secondary is in a anti-clockwise sense and the z-axis is orientated out of the plane of the paper. The lower panels depict the system as viewed from the x-z plane. In each case a half-Gaussian distribution for  $k$  was used: to reflect a stream of blobs with a dense core and tenuous wings (higher  $k$  values). The distribution mean and standard deviation were  $t_{\text{mag}}(L_1)/t_{\text{dyn}}(L_1) = 0.25$  and  $0.025$  (tailing to lower values) respectively. The left-hand panels show the results of a simulation which also includes an equal number of particles with very low  $k$  values, in order to demonstrate the robust nature of the spin equilibrium (see section 2).

**Figure 2** A sequence of views of the accretion flow in the equilibrium state for a simulation with magnetic parameters equal to those of the right-hand panels of figure 1. The left hand panels in the figure show the x-y projection of the system, while the right-hand panels show the corresponding x-z projection. Each set of panels are separated in time by  $0.2 P_{\text{orb}}$ .

**Figure 3** Fractions of mass transferred through  $L_1$  which are accreted by the white dwarf (solid curve), recaptured by the secondary star (dot-dash curve), and escaping from the binary (dashed curve), for the simulation shown in figure 2.

**Figure 4** As figure 2, but for a simulation with magnetic parameters equal to those of the simulation shown in the left-hand panels of figure 1.

**Figure 5** Equilibrium  $P_{\text{spin}}/P_{\text{orb}}$  values as a function of

$t_{\text{mag}}(L_1)/t_{\text{dyn}}(L_1)$ , and estimated  $\mu_1$  for EX Hya.

**Figure 6**  $t_{\text{mag}}(L_1)/t_{\text{dyn}}(L_1)$  versus  $P_{\text{orb}}$ . From top to bottom the panels plot the time-scales for  $\mu_1 = 10^{33}$ ,  $2 \times 10^{33}$ ,  $4 \times 10^{33}$  G cm<sup>3</sup>.

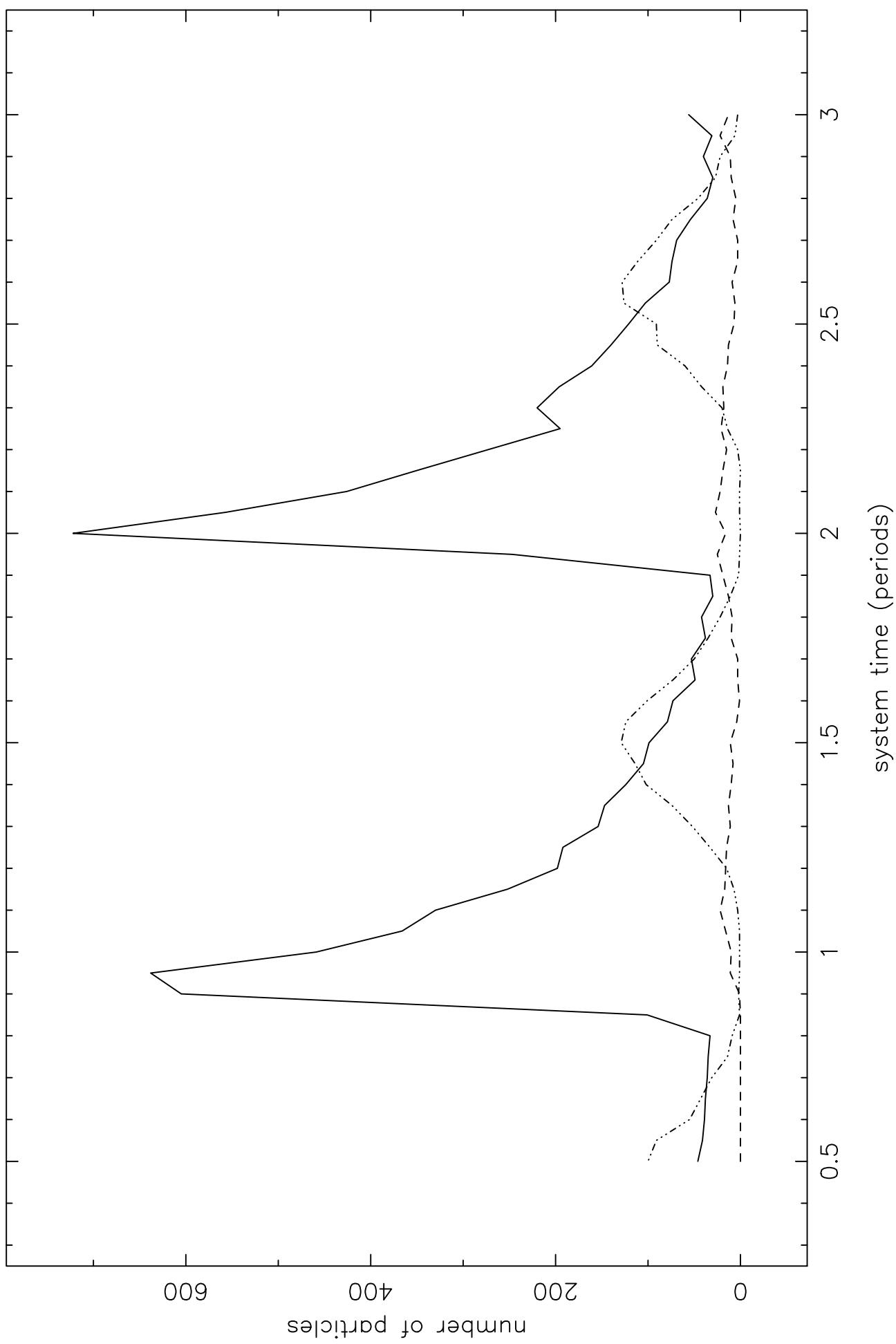
**Figure 7** Schematic classification of magnetic CVs according to  $\mu_1$  and  $P_{\text{orb}}$ . Here DQ Her systems are taken to represent systems which accrete via a Keplerian disc and have  $P_{\text{spin}}/P_{\text{orb}} \ll 0.07$ .

This figure "figure1.gif" is available in "gif" format from:

<http://arxiv.org/ps/astro-ph/9909312v1>

This figure "figure2.gif" is available in "gif" format from:

<http://arxiv.org/ps/astro-ph/9909312v1>





This figure "figure4.gif" is available in "gif" format from:

<http://arxiv.org/ps/astro-ph/9909312v1>

